



# CHORUS

This is the accepted manuscript made available via CHORUS. The article has been published as:

## Are There Sterile Neutrinos at the eV Scale?

Joachim Kopp, Michele Maltoni, and Thomas Schwetz

Phys. Rev. Lett. **107**, 091801 — Published 23 August 2011

DOI: [10.1103/PhysRevLett.107.091801](https://doi.org/10.1103/PhysRevLett.107.091801)

## Are there sterile neutrinos at the eV scale?

Joachim Kopp,<sup>1</sup> Michele Maltoni,<sup>2</sup> and Thomas Schwetz<sup>3</sup>

<sup>1</sup>*Fermilab, Theoretical Physics Department, PO Box 500, Batavia, IL 60510, USA*

<sup>2</sup>*Instituto de Física Teórica UAM/CSIC, Calle de Nicolás Cabrera 13-15, E-28049 Madrid, Spain*

<sup>3</sup>*Max-Planck-Institut für Kernphysik, PO Box 103980, 69029 Heidelberg, Germany*

New predictions for the anti-neutrino flux from nuclear reactors suggest that reactor experiments may have measured a deficit in this flux, which can be interpreted in terms of oscillations between the known active neutrinos and new sterile states. We perform a re-analysis of global short-baseline neutrino oscillation data in a framework with one or two sterile neutrinos. While one sterile neutrino is still not sufficient to reconcile the signals suggested by reactor experiments and by the LSND and MiniBooNE experiments with null results from other searches, we find that, with the new reactor flux prediction, the global fit improves considerably when two sterile neutrinos are introduced.

PACS numbers: 14.60.Pq, 14.60.St

**Introduction.** By now a standard paradigm of neutrino physics has emerged. A beautiful series of experiments has established the phenomenon of neutrino oscillations. Results from solar, atmospheric, reactor, and accelerator neutrino experiments can be accommodated nicely by oscillations of the three neutrinos of the Standard Model, the so-called “active” neutrinos, with mass-squared differences of order  $10^{-4}$  and  $10^{-3}$  eV<sup>2</sup>, see [1, 2] for recent fits and references. There are, however, a few experimental results which cannot be explained within this framework and seem to require additional neutrinos with masses at the eV scale [3, 4]. Such neutrinos cannot participate in the weak interactions due to collider constraints, and are therefore called “sterile” neutrinos.

Recently another hint for sterile neutrinos has emerged from a re-evaluation of the expected electron anti-neutrino ( $\bar{\nu}_e$ ) flux emitted by nuclear reactors [5]. The new prediction is  $\sim 3\%$  higher than what was previously assumed [6]. If confirmed, this result would imply that all existing neutrino oscillation searches at nuclear reactors have observed a deficit of  $\bar{\nu}_e$ , which can be interpreted in terms of oscillations at baselines of order 10–100 m [7]. At typical reactor anti-neutrino energies of few MeV, standard oscillations of the three active neutrinos require baselines of a least 1 km. Hence, the “reactor anomaly” can only be accommodated if at least one sterile neutrino with mass at the eV-scale or higher is introduced. This is particularly intriguing because also the long-standing “LSND anomaly” [3], as well as the more recent MiniBooNE anti-neutrino results [4] suggest the existence of a sterile neutrino in that mass range.

Previous phenomenological studies [8–10] have been performed in a framework in which the standard three active neutrino scenario is amended by adding one (“3+1”) or two (“3+2”) sterile neutrinos with masses at the eV scale. These studies came to the conclusion that an explanation of the aforementioned anomalies within these sterile neutrino scenarios is in conflict with various constraints from other neutrino oscillation searches at short baselines (SBL), including also data from reactor exper-

	$\Delta m_{41}^2$ [eV <sup>2</sup> ]	$ U_{e4} $	$\Delta m_{51}^2$ [eV <sup>2</sup> ]	$ U_{e5} $	$\chi^2/\text{dof}$
3+1	1.78	0.151			50.1/67
3+2	0.46	0.108	0.89	0.124	46.5/65

**Table I:** Best fit points for the 3+1 and 3+2 scenarios from reactor anti-neutrino data. The total number of data points is 69 (Bugey3 spectra plus 9 SBL rate measurements; we have omitted data from Chooz and Palo Verde, which are not very sensitive to the model parameters, but would dilute the  $\chi^2$  by introducing 15 additional data points). For no oscillations we have  $\chi^2/\text{dof} = 59.0/69$ .

iments. In this note we revisit 3+1 and 3+2 sterile neutrino oscillation schemes in the light of the new reactor neutrino fluxes. We argue that one sterile neutrino is still not sufficient to describe all data, whereas a 3+2 framework is now in much better agreement with the data.

**Fit of SBL reactors.** Let us first discuss the implications of the new reactor anti-neutrino flux prediction for reactor data alone by analyzing a set of SBL reactor experiments at baselines  $L \lesssim 100$  m [7]. We include full spectral data from the Bugey3 experiment [11] at 15, 40 and 95 m and take into account the Bugey4 [12], ROVNO [13], Krasnoyarsk [14], ILL [15], and Gösigen [16] experiments via the rate measurements summarized in Table II of [7]. Furthermore we include the Chooz [17] and Palo Verde [18] experiments at  $L \simeq 1$  km. We use the neutrino fluxes from the isotopes <sup>235</sup>U, <sup>239</sup>Pu, <sup>238</sup>U, <sup>241</sup>Pu obtained in [5] and we include the uncertainty on the integrated flux for each isotope given in Table I of [7], correlated between all experiments. For further technical details see [1].

We perform a fit to these data within the 3+1 and 3+2 sterile neutrino frameworks, where neutrino oscillations for SBL reactor experiments depend on 2 and 4 parameters, respectively. The parameters are the mass-squared differences  $\Delta m_{41}^2$  and  $\Delta m_{51}^2$  between the eV-scale sterile neutrinos and the light neutrinos, and the elements  $|U_{e4}|$  and  $|U_{e5}|$  of the leptonic mixing matrix, which de-

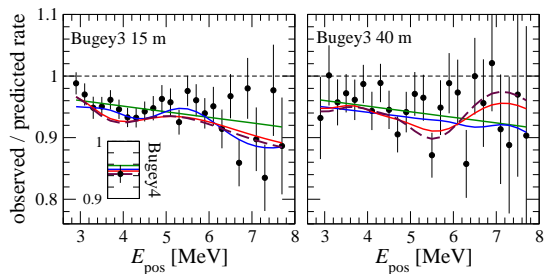


**Figure 1:** Comparison of sterile neutrino models to reactor data: energy spectra from Bugey3 and the rate measurement of Bugey4 (inset). The data points show the ratio of the observed and predicted event numbers where the prediction is based on the new reactor anti-neutrino fluxes [5] and does not include oscillations. Bugey3 error bars are statistical only, whereas the error on the Bugey4 rate is dominated by systematics. The green solid curve shows the prediction for the no oscillation hypothesis, the blue solid and red solid curves correspond to the 3+1 and 3+2 best fit points for SBL reactor data (Tab. I), and the dashed curve corresponds to the 3+2 best fit point of global SBL data (Tab. II).

scribe the mixing of the electron neutrino flavor with the heavy neutrino mass states  $\nu_4$  and  $\nu_5$ . Obviously, for the 3+1 case, only  $\nu_4$  is present. The best fit points for the two scenarios are summarized in Tab. I. To illustrate the impact of sterile neutrinos on the fit to reactor anti-neutrino data graphically, we compare in Fig. 1 the data to the predictions for the no oscillation case (green) and the best fit 3+1 (blue) and 3+2 (red) models. Note that, even for no oscillations, the prediction may deviate from 1 due to nuisance parameters included in the fit to parametrize systematic uncertainties. The fit is dominated by Bugey3 spectral data at 15 m and 40 m and the precise rate measurement from Bugey4.

In the lower part of Fig. 2 we show the  $\chi^2$  of the SBL reactor fit as a function of  $\Delta m_{41}^2$ . Using the new flux predictions (solid curves) we find a clear preference for sterile neutrino oscillations: the  $\Delta\chi^2$  between the no oscillation hypothesis and the 3+1 best fit point is 8.5, which implies that the no oscillation case is disfavored at about 98.6% CL (2 dof). In the 3+2 case the no oscillation hypothesis is disfavored compared to the 3+2 best fit point with  $\Delta\chi^2 = 12.1$ , or 98.3% CL (4 dof). In contrast, with previous flux predictions (dashed curves) the improvement of the fit is not significant, with a  $\Delta\chi^2$  between the best fit points and the no oscillation case of only 3.6 and 4.4 for the 3+1 and 3+2 hypotheses, respectively.

**Global analysis of SBL data.** The constraints from the reactor experiments under discussion play an important role in a combined analysis of all SBL oscillation data, including the LSND and MiniBooNE anomalies. LSND has provided evidence for  $\bar{\nu}_\mu \rightarrow \bar{\nu}_e$  transitions [3], and MiniBooNE has reported an excess of events in the same channel, consistent with the LSND signal [4]. This hint for oscillations is however not confirmed by a Mini-

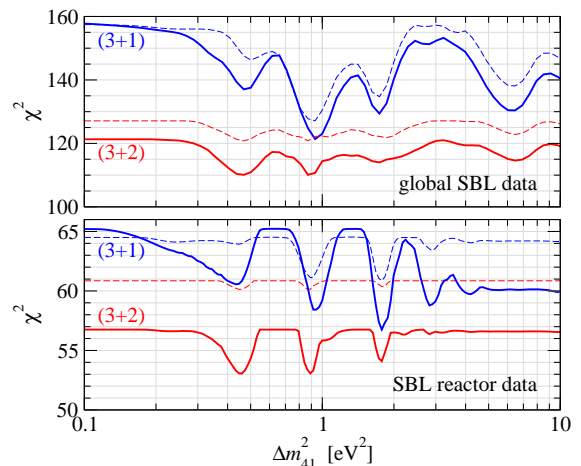


**Figure 2:**  $\chi^2$  from global SBL data (upper panel) and from SBL reactor data alone (lower panel) for the 3+1 (blue) and 3+2 (red) scenarios. Dashed (solid) curves were computed using the old [6] (new [5]) reactor  $\bar{\nu}_e$  flux prediction. All undisplayed parameters are minimized over. The total number of data points is 137 (84) for the global (reactor) analysis.

BooNE search in the  $\nu_\mu \rightarrow \nu_e$  channel [19], where the data in the energy range sensitive to oscillations is consistent with the background expectation. These results seem to suggest an explanation involving CP violation in order to reconcile different results for neutrino and anti-neutrino searches. An explanation of the LSND and MiniBooNE anomalies via sterile neutrino oscillations requires the mixing matrix elements  $|U_{e4}|$  and/or  $|U_{e5}|$  to be non-zero. Reactor experiments are sensitive to these parameters, and while analyses using previous flux predictions lead to tight constraints on them, the new fluxes imply non-zero best fit values (Tab. I) and closed allowed regions at 98% CL. Hence, the interesting question arises whether a consistent description of the global data on SBL oscillations (including LSND/MiniBooNE) becomes now possible. To answer this question we perform a fit by including, in addition to the reactor searches for  $\bar{\nu}_e$  disappearance, the LSND [3] and MiniBooNE [4, 19] results, as well as additional constraints from appearance experiments [20, 21],  $\nu_\mu$  disappearance searches [22], and atmospheric neutrinos. Technical details of our analysis can be found in [8, 10] and references therein.

In the 3+1 scheme the SBL experiments depend on the three parameters  $\Delta m_{41}^2$ ,  $|U_{e4}|$ , and  $|U_{\mu 4}|$ . Since only one mass scale is relevant in this case it is not possible to obtain CP violation. Therefore, oscillations involving one sterile neutrino are not capable of reconciling the different results for neutrino (MiniBooNE) and anti-neutrino (LSND and MiniBooNE) appearance searches. Fig. 3 compares the allowed regions from LSND and MiniBooNE anti-neutrino data to the constraints from the other experiments in the 3+1 model. Note that, even though reactor analyses using the new flux predic-

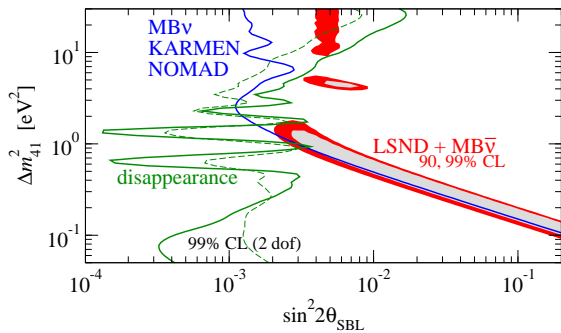


**Figure 3:** Global constraints on sterile neutrinos in the 3+1 model. We show the allowed regions at 90% and 99% CL from a combined analysis of the LSND [3] and MiniBooNE anti-neutrino [4] signals (filled regions), as well as the constraints from the null results of KARMEN [20], NOMAD [21] and MiniBooNE neutrino [19] appearance searches (blue contour). The limit from disappearance experiments (green contours) includes data from CDHS [22], atmospheric neutrinos, and from the SBL reactor experiments. For the latter we compare results obtained using the new  $\bar{\nu}_e$  flux prediction [5] (solid) to those obtained using the previous prediction [6] (dashed). The region to the right of the curves is excluded at 99% CL.

	$\Delta m_{41}^2$	$ U_{e4} $	$ U_{\mu 4} $	$\Delta m_{51}^2$	$ U_{e5} $	$ U_{\mu 5} $	$\delta/\pi$	$\chi^2/\text{dof}$
3+2	0.47	0.128	0.165	0.87	0.138	0.148	1.64	110.1/130
1+3+1	0.47	0.129	0.154	0.87	0.142	0.163	0.35	106.1/130

**Table II:** Parameter values and  $\chi^2$  at the global best fit points for 3+2 and 1+3+1 oscillations ( $\Delta m^2$ 's in  $\text{eV}^2$ ).

tion prefer non-zero  $U_{e4}$ , no closed regions appear for the disappearance bound (solid curve), since  $\sin^2 2\theta_{\text{SBL}} = 4|U_{e4}|^2|U_{\mu 4}|^2$  can still become zero if  $U_{\mu 4} = 0$ . We find that the parameter region favored by LSND and MiniBooNE anti-neutrino data is ruled out by other experiments, except for a tiny overlap of the three 99% CL contours around  $\Delta m_{41}^2 \approx 1 \text{ eV}^2$ . Note that in this region the constraint from disappearance data does not change significantly due to the new reactor flux predictions. Using the PG test from [23] we find a compatibility of the LSND+MiniBooNE( $\bar{\nu}$ ) signal with the rest of the data only of about  $10^{-5}$ , with  $\chi_{\text{PG}}^2 = 21.5(24.2)$  for new (old) reactor fluxes. Hence we conclude that the 3+1 scenario does not provide a satisfactory description of the data despite the new hint coming from reactors.

Let us move now to the 3+2 model, where SBL experiments depend on the seven parameters listed in Tab. II. In addition to the two mass-squared differences and the moduli of the mixing matrix elements, also a physical complex phase enters,  $\delta \equiv \arg(U_{\mu 4}U_{e4}^*U_{\mu 5}^*U_{e5})$ . This phase leads to CP violation in SBL oscillations [8, 24], allowing to reconcile differing neutrino and anti-neutrino results from MiniBooNE/LSND. Tab. II shows the parameter values at the global best fit point and the cor-

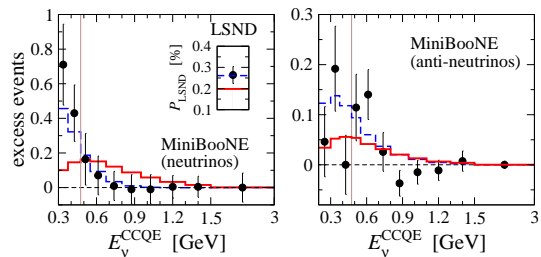


**Figure 4:** Predicted spectra for MiniBooNE data and the transition probability for LSND (inset). Solid histograms refer to the 3+2 global best fit point (Tab. II), dashed histograms correspond to the best fit of appearance data only (LSND, MiniBooNE  $\nu/\bar{\nu}$ , KARMEN, NOMAD). For MiniBooNE we fit only data above 475 MeV.

responding  $\chi^2$  value. Changing from the previous to the new reactor flux calculations the  $\chi^2$  decreases by 10.6 units, indicating a significant improvement of the description of the data, see also upper panel of Fig. 2. From that figure follows also that going from 3+1 to 3+2 leads to a significant improvement of the fit with the new reactor fluxes, which was not the case with the old ones. The  $\chi^2$  improves by 11.2 units, which means that 3+1 is disfavored at the 97.6% CL (4 dof) with respect to 3+2, compared to  $\Delta\chi^2 = 6.3$  (82% CL) for old fluxes.

In Fig. 1 we show the prediction for the Bugey spectra at the global best fit point as dashed curves. Clearly they are very similar to the best fit of reactor data only. Fig. 4 shows the predicted spectra for MiniBooNE neutrino and anti-neutrino data, as well as the LSND  $\bar{\nu}_\mu \rightarrow \bar{\nu}_e$  transition probability. Again we find an acceptable fit to the data, although in this case the fit is slightly worse than a fit to appearance data only (dashed histograms). Note that MiniBooNE observes an event excess in the lower part of the spectrum. This excess can be explained if only appearance data are considered, but not in the global analysis including disappearance searches [8]. Therefore, we follow [19] and assume an alternative explanation for this excess, e.g. [25]. In Tab. III we show the compatibility of the LSND/MiniBooNE( $\bar{\nu}$ ) signal with the rest of the data, as well as the compatibility of appearance and disappearance searches using the PG test from [23]. Although the compatibility improves drastically when changing from old to new reactor fluxes, the PG is still below 1% for 3+2. This indicates that some tension between data sets remains. We considered also a “1+3+1” scenario, in which one of the sterile mass eigenstates is lighter than the three active ones and the other is heavier [26]. As can be seen from Tabs. II and III the fit of 1+3+1 is slightly better than 3+2, with  $\Delta\chi^2 = 15.2$  between 3+1 and 1+3+1 (99.6% CL for 4 dof). However, due to the larger total mass in neutrinos, a 1+3+1 ordering might be in more tension with cosmology than a 3+2 scheme [27–29]. Fig. 5 shows the allowed regions for the two eV-scale mass-squared differences for the 3+2

	LSND+MB( $\bar{\nu}$ ) vs rest appearance vs disapp.			
	old	new	old	new
$\chi^2_{\text{PG},3+2}/\text{dof}$	25.1/5	19.9/5	19.9/4	14.7/4
PG <sub>3+2</sub>	$10^{-4}$	0.13%	$5 \times 10^{-4}$	0.53%
$\chi^2_{\text{PG},1+3+1}/\text{dof}$	19.6/5	16.0/5	14.4/4	10.6/4
PG <sub>1+3+1</sub>	0.14%	0.7%	0.6%	3%

**Table III:** Compatibility of data sets [23] for 3+2 and 1+3+1 oscillations using old and new reactor fluxes.

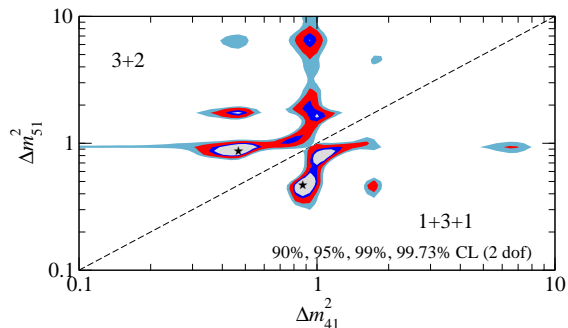


**Figure 5:** The globally preferred regions for the neutrino mass squared differences  $\Delta m^2_{41}$  and  $\Delta m^2_{51}$  in the 3+2 (upper left) and 1+3+1 (lower right) scenarios.

and 1+3+1 schemes.

**Discussion.** Let us comment briefly on other signatures of eV-scale sterile neutrinos. We have checked the fit of solar neutrino data and the KamLAND reactor experiment, and found excellent agreement. The effect of non-zero  $U_{e4}$  and  $U_{e5}$  for these data are similar to the one of  $U_{e3}$  in the standard three-active neutrino case, and hence the 3+2 best fit point mimics a non-zero  $U_{e3}$  close to the preferred value of these data, see [1, 2, 30]. Our best-fit points also fall in the range of parameter values required to explain the small  $\nu_e$  deficit observed in radioactive source measurements at radiochemical neutrino detectors [31]. The MINOS long-baseline experiment has performed a search for sterile neutrinos via neutral current (NC) measurements [32]. We have estimated that the best fit points reported in Tab. II lead to an increase of the  $\chi^2$  of MINOS NC data as well as  $\chi^2_{\text{PG}}$  by a few units [30]. Finally, sterile neutrinos may manifest themselves in cosmology. Recent studies [27–29] indicate a slight preference for extra radiation content in the universe (mainly from CMB measurements), favoring the existence of light sterile neutrinos. On the other hand, Big-Bang nucleosynthesis constrains the number of extra neutrino species to be  $< 1.2$  at 95% CL [33], which may be a challenge for two-sterile neutrino schemes. Moreover, global fits to cosmological data constrain the sum of the neutrino masses to be  $\leq 0.7$  to  $1.5$  eV at 95% CL [27–29], depending on the used data, whereas our 3+2 best

fit point leads to  $\sum m_\nu \approx 1.7$  eV. Hence, sterile neutrino explanations of short-baseline oscillation data are in tension with cosmology, or, if confirmed, would indicate a deviation from the standard cosmological picture.

In conclusion, we have shown that a global fit to short-baseline oscillation searches assuming two sterile neutrinos improves significantly when new predictions for the reactor neutrino flux are taken into account, although some tension remains. We are thus facing an intriguing accumulation of hints for the existence of sterile neutrinos at the eV scale, and a confirmation of these hints in the future would certainly be considered a major discovery.

**Acknowledgments.** This work was supported by the US Department of Energy (DE-AC02-07CH11359), the Spanish MICINN (FPA-2009-08958, FPA-2009-09017, CSD-2008-0037), the Comunidad Autnoma de Madrid (HEPHACOS S2009/ESP-1473), the Deutsche Forschungsgemeinschaft, and the European Union (EURO $\nu$ ).

- [1] T. Schwetz, M. Tortola, and J. W. F. Valle, (2011), 1103.0734.
- [2] M. C. Gonzalez-Garcia *et al.*, JHEP **04**, 056 (2010).
- [3] A. Aguilar *et al.*, Phys. Rev. **D64**, 112007 (2001).
- [4] A. A. Aguilar *et al.*, Phys. Rev. Lett. **105**, 181801 (2010).
- [5] T. A. Mueller *et al.*, (2011), 1101.2663.
- [6] K. Schreckenbach *et al.*, Phys.Lett. **B160**, 325 (1985).
- [7] G. Mention *et al.*, (2011), 1101.2755.
- [8] M. Maltoni and T. Schwetz, Phys. Rev. **D76**, 093005 (2007).
- [9] G. Karagiorgi *et al.*, Phys.Rev. **D80**, 073001 (2009).
- [10] E. Akhmedov and T. Schwetz, JHEP **1010**, 115 (2010).
- [11] Y. Declais *et al.*, Nucl.Phys. **B434**, 503 (1995).
- [12] Y. Declais *et al.*, Phys.Lett. **B338**, 383 (1994).
- [13] A. Kuvshinnikov *et al.*, JETP Lett. **54**, 253 (1991).
- [14] G. Vidyakin *et al.*, Sov.Phys.JETP **66**, 243 (1987).
- [15] H. Kwon *et al.*, Phys.Rev. **D24**, 1097 (1981).
- [16] G. Zacek *et al.*, Phys.Rev. **D34**, 2621 (1986).
- [17] M. Apollonio *et al.*, Eur. Phys. J. **C27**, 331 (2003).
- [18] F. Boehm *et al.*, Phys.Rev. **D64**, 112001 (2001).
- [19] A. Aguilar *et al.*, Phys.Rev.Lett. **98**, 231801 (2007).
- [20] B. Armbruster *et al.*, Phys. Rev. **D65**, 112001 (2002).
- [21] P. Astier *et al.*, Nucl. Phys. **B611**, 3 (2001).
- [22] F. Dydak *et al.*, Phys. Lett. **B134**, 281 (1984).
- [23] M. Maltoni and T. Schwetz, Phys. Rev. **D68**, 033020 (2003).
- [24] G. Karagiorgi *et al.*, Phys. Rev. **D75**, 013011 (2007).
- [25] R. J. Hill, (2010), 1002.4215.
- [26] S. Goswami and W. Rodejohann, JHEP **10**, 073 (2007).
- [27] M. C. Gonzalez-Garcia *et al.*, JHEP **08**, 117 (2010).
- [28] J. Hamann *et al.*, Phys. Rev. Lett. **105**, 181301 (2010).
- [29] E. Giusarma *et al.*, (2011), 1102.4774.
- [30] J. Kopp, M. Maltoni, and T. Schwetz, work in progress.
- [31] M. A. Acero *et al.*, Phys. Rev. **D78**, 073009 (2008).
- [32] P. Adamson *et al.*, Phys.Rev. **D81**, 052004 (2010).
- [33] G. Mangano and P. D. Serpico, (2011), 1103.1261.